Proceedings of the 1st Global Power and Propulsion Forum
GPPF 2017
Jan 16-18, 2017, Zurich, Switzerland
www.pps.global

GPPF-2017-113

DEVELOPMENT OF A HIGHLY EFFICIENT DENSITY-BASED SOLVER FOR CONDENSING STEAM FLOWS IN TURBOMACHINES

Pascal Post
Energy and Power Plant Technology
Technische Universität Darmstadt
post@ekt.tu-darmstadt.de
Darmstadt, Germany

Francesca di Mare
Energy and Power Plant Technology
Technische Universität Darmstadt
dimare@ekt.tu-darmstadt.de
Darmstadt, Germany

ABSTRACT

In this paper an extension of the German Aerospace Center's (DLR) in-house density-based turbomachinery CFD code TRACE for the efficient, accurate, consistent and robust computation of condensing steam flows is presented. The properties of this novel approach are achieved by a consistent and uniform formulation of the state equations eminently suitable for density-based CFD solvers and a compatible, efficient and accurate tabular approach to the description of the thermodynamic and transport properties of the working fluid.

The latter is realized by utilizing the Spline Based Table Lookup (SBTL) [1] method, that has been developed especially for this purpose. The solution method is developed based on a consistent generalization of the functional expression of the state equation which permits an extension of the numerical treatment starting from the ideal gas case. The numerical fluxes are assembled using a generalized Roe-type scheme, representing a clear innovation for the wet steam flow considered in this work, where an equilibrium assumption is invoked in the two-phase region at present time. In addition, a true real-gas extension of the non-reflecting boundary treatment of Saxer and Giles [2] is proposed.

Capabilities and potential of the newly developed real-gas steam solver are demonstrated comparing to both, the industrial standard formulation IAPWS-IF97 [3] and ideal gas calculations in three different configurations, a de Laval nozzle geometry, a quasi-3D cascade and an idealized 3D cascade geometry. Overall, results indicate a significant speed-up and an increased robustness compared to the current industrial standard retaining its accuracy at the same time.

While matching the accuracy of the IAPWS-IF97 formulation, the new approach allows computations to be overall about 4.6 times faster (in case of a de Laval nozzle, for example). Due to these qualities, the developed solver has the potential for high-performance computations adopting Large-eddy simulations of wet and condensing steam, which are now running for the first time.

INTRODUCTION

In many industrial fluid flows, real-gas effects play a key role such as, for example, in steam turbines where insight into the aero-thermal interactions within the complex transient 3D multi-phase flow involving real-gas effects must be gained for effective optimization of the processes. This goal can be achieved by means of efficient and fast computational techniques capable of accounting for these challenging phenomena.

Over the last years 3D pressure-based [4, 5] as well as density-based [6, 7] solver for condensing steam flows have been developed based on adaptions of the virial equation of state. This paper provides the extension of the in-house density-based turbomachinery CFD code TRACE [8] to efficiently, accurately, consistently and robustly calculate condensing steam flows in turbomachines utilizing a novel general equation of state approach and the Spline Based Table Lookup (SBTL) [1] method. The governing mathematical model is described first. The solution method is presented next, where the necessary and challenging extension of the employed Roe-scheme to real-gas and steam applications plays a central role.

Whilst in the case of an ideal gas it is sufficient to find velocity and total enthalpy of the Roe-averaged state, for the more general system considered the Roe-type linearization is no longer uniquely determined, as the number of explicitly occurring quantities in the flux Jacobian exceeds the number of conditions defining the Roe-type linearization and the construction by a parameter vector is no longer available. Several approaches to generalize the Roe-type linearization have been proposed [9, 10].

Most of them drop the idea of a Roe-averaged state and instead define Roe-averaged quantities which are additional independent unknowns of the linearization process without thermodynamic significance [10]. This can lead to

inconsistencies, whenever these quantities are employed to derive other thermodynamic variables such as the speed of sound and, especially in two-phase flows, to a non-hyperbolic linearization [11]. In our experience these methods lead to unphysical intermediate states as soon as condensation occurs.

To overcome this issue, the approach of Cinnella [10], based in turn on the idea presented in [12], is followed here. Corresponding to the ideal gas approach, a Roe-averaged state is searched, such that the occurring partial derivatives are now considered as depended unknowns evaluated at the intermediate state, which is constructed by direct substitution into Roe's [13] conservation property. The resulting system is under-determined and the number of additionally required constraints depends on the particular choice of the pressure equation of state.

In addition to requiring the generalized Roe-averaged state to naturally reduce to the ideal gas case, Cinnella [10] follows the approach of Liou et al. [14], but proposes to omit the projection over the straight line. This projection might not lead to a physically consistent state for a two-phase flow [11], as also confirmed from our experience. Omitting the system with the general equation of state satisfies the conservation property only to within $\mathcal{O}\left(\|\Delta \underline{w}\|^2\right)$, rendering the linearization not a true Roe-type linearization. In a second order scheme, the accepted error is of order $\mathcal{O}\left(\delta x^6\right)$, with δx being the mesh size, and results indicate that this error does not significantly affect the computational outcomes while enhancing the performance [10].

In addition, the boundary treatment for the considered general equation of state is addressed, including a real-gas extension of the non-reflecting boundary treatment of Saxer and Giles [2]. Finally, the capabilities and potential of the newly developed real-gas steam solver are demonstrated in a de Laval nozzle configuration, a quasi-3D cascade and an idealized 3D-extension of the cascade geometry.

MATHEMATICAL MODEL

The three-dimensional Navier-Stokes equations in conservative form are solved

$$\partial_t \underline{w} + \operatorname{div}\left(\underline{\underline{F}}^a + \underline{\underline{F}}^d\right) = \underline{0}\,. \tag{1}$$

The vector of unknowns comprises the conservative variables, density, specific momentum and total internal energy

$$\underline{w}(\underline{x},t) := \left(\rho, \underline{\varpi}, \varepsilon_t\right)^{\mathrm{T}} := \left(\rho, \rho\underline{u}, \rho e_t\right)^{\mathrm{T}},$$

with the convective and diffusive fluxes defined as

$$\underline{\underline{F}}^a(\underline{w}) := \left(\rho\underline{u},\ \rho\underline{u}\otimes\underline{u} + p\underline{\underline{I}},\ \rho\underline{u}h_t\right)$$
$$\underline{\underline{F}}^d(\underline{w}) := \left(\underline{0}, -\underline{\underline{\tau}},\ \underline{q} - \underline{u}\cdot\underline{\tau}\right),$$

where $\underline{\underline{I}}$ is the identity tensor. Total internal energy and enthalpy are defined as

$$\left(e_t, h_t\right) := \left(e, h\right) + \tfrac{1}{2}\underline{u}\cdot\underline{u}$$

the specific enthalpy by

$$h := e + \rho^{-1}p\,.$$

As density and internal energy can directly be calculated from the conservative variables without the need of a thermodynamic equation of state, it is most efficient and consistent to choose these as the independent thermodynamic state variables in our solution method. Thus, for the thermodynamic pressure p, which must be a function of the conservative variables $p = p(\underline{w})$ by definition, following generalized equation of state is adopted for system (1)

$$p := p(\rho, e) = p\left(\rho, \rho^{-1}\varepsilon_t - \left(2\rho^2\right)^{-1}\underline{\varpi}\cdot\underline{\varpi}\right).$$

In the proposed solution method the latter is provided in tabular form by the SBTL functions [1]. Assuming a Newtonian fluid in combination with Stokes' relation and with Fourier's law, the viscous shear stress tensor and heat flux vector are given by

$$\underline{\underline{\tau}}(\underline{w}) := \eta(\rho, e)\left(\operatorname{grad}\underline{u} + \left(\operatorname{grad}\underline{u}\right)^{\mathrm{T}} - \tfrac{2}{3}\operatorname{div}\underline{u}\,\underline{\underline{I}}\right)$$
$$\underline{q}(\underline{w}) := -\lambda(\rho, e)\ \operatorname{grad}T(\rho, e).$$

Temperature $T(\rho,e)$, molecular viscosity $\eta(\rho,e)$ and thermal conductivity coefficient $\lambda(\rho,e)$ are again tabulated using the SBTL method [1].

For condensing steam an equilibrium assumption (homogeneous equilibrium mixture model) is invoked in the two-phase region at present time and no condensation model is incorporated in the first instance. This treatment describing the conservation of mixture quantities in the saturated liquid-vapor mixture region retains the general structure of the governing equations (1). With subscripts for saturated liquid $(\bullet)_l$ and vapor $(\bullet)_v$ the properties of the mixture $(\bullet)_m$ are given by

$$\left(h, e, s\right)_m = \left(1-x\right)\left(h, e, s\right)_l + x\left(h, e, s\right)_v$$
$$\rho_m = \left(1-\alpha\right)\rho_l + \alpha\,\rho_v,$$

where x and α represent respectively mass and volume fraction of steam in the wet steam mixture. Speed of sound, molecular viscosity and thermal conductivity coefficient of the mixture are given by

$$\left(a, \eta, \lambda\right)_m := \left(1-\alpha\right)\left(a, \eta, \lambda\right)_l + \alpha\left(a, \eta, \lambda\right)_v.$$

The Favre-averaged conservation equations are solved and turbulence is modelled according to a classic RANS approach based on the two-equation k-ω model [15]. The conservative variables of eq. (1) are then given by $\underline{w} := \left(\overline{\rho}, \overline{\rho}\widetilde{\underline{u}}, \overline{\rho}\widetilde{e}_t\right)^{\mathrm{T}}$, the corresponding fluxes by

$$\underline{\underline{F}}^a(\underline{w}) = \left(\overline{\rho}\widetilde{\underline{u}},\ \overline{\rho}\widetilde{\underline{u}}\otimes\widetilde{\underline{u}} + \overline{p}\underline{\underline{I}},\ \overline{\rho}\widetilde{\underline{u}}\widetilde{h}_t\right)$$
$$\underline{\underline{F}}^d(\underline{w}) \approx \left(\underline{0}, -\underline{\underline{\tau}}^*, \underline{q}^* - \widetilde{\underline{u}}\cdot\underline{\underline{\tau}}^*\right).$$

The Boussinesq approximation [16] is invoked, so that the total stresses (turbulent and viscous) and heat fluxes read

$$\underline{\underline{\tau}}^* :\approx \left(\eta\left(\overline{\rho}, \widetilde{e}\right) + \eta^t\right)\left(\operatorname{grad}\widetilde{\underline{u}} + \left(\operatorname{grad}\widetilde{\underline{u}}\right)^{\mathrm{T}} - \tfrac{2}{3}\operatorname{div}\widetilde{\underline{u}}\,\underline{\underline{I}}\right)$$
$$\underline{q}^* :\approx -\left(\lambda\left(\overline{\rho}, \widetilde{e}\right) + \lambda^t\right)\ \operatorname{grad}T\left(\overline{\rho}, \widetilde{e}\right).$$

The turbulent thermal conductivity coefficient λ^t is computed based on a constant turbulent Prandtl-number equal to 0.9. The influence of the turbulent kinetic energy on the Favre-averaged total internal energy and enthalpy is presently neglectedwith negligible impact on the results

$$\left(\tilde{e}_t, \tilde{h}_t\right) \approx \left(\tilde{e}, \tilde{h}\right) + \tfrac{1}{2}\underline{\tilde{u}} \cdot \underline{\tilde{u}}.$$

Much more involved Large-eddy simulations are currently in progress.

SOLUTION METHOD

The governing equations (1) are spatially discretized using a finite volume approach [17], the diffusive fluxes are discretized using central differences on a boundary fitted curvilinear coordinates mesh [8].

For the steady state computations shown in the present work, the ordinary differential equations are integrated in pseudo time employing an Euler-backward scheme. The occurring numerical fluxes at the new time step are linearized about the current time step as described in [18]. The resulting viscous flux Jacobians are implemented based on [19] and need only minor adaptions for the generalized equations of state (1). The linear system of algebraic equations is then solved by the Gauss-Seidel method.

The convective fluxes are discretized by a second order accurate Roe-type scheme. Basis for this is an extension of Godunov's scheme [20] to three dimensions assuming the inter-cell boundaries to be infinite planes, separating the two constant states $\underline{w}_i$ and $\underline{w}_j$. In a local, face normal coordinate system defined by the outward unit normal vector of the inter-cell boundary $\hat{\underline{n}}_{ij}$, this results in a (augmented) 1D Riemann problem

$$\left.\begin{aligned} \partial_t \underline{w} + \partial\left(\hat{\underline{n}}_{ij} \cdot \underline{\underline{F}}^a\right) \big/ \partial\left(\hat{\underline{n}}_{ij} \cdot \underline{x}\right) &= \underline{0} \\ \underline{w}\left(\hat{\underline{n}}_{ij} \cdot \underline{x}, t\right)\Big|_{t=t_0} &= \begin{cases} \underline{w}_i\,, \hat{\underline{n}}_{ij} \cdot \underline{x} < 0 \\ \underline{w}_j\,, \hat{\underline{n}}_{ij} \cdot \underline{x} < 0 \end{cases} \end{aligned}\right\}, \tag{2}$$

solved approximately introducing a Roe type linearization.

By defining

$$\begin{aligned} \partial_t \underline{w} + \underline{\underline{A}}\left(\underline{w}, \hat{\underline{n}}_{ij}\right) \partial \underline{w} \big/ \partial\left(\hat{\underline{n}}_{ij} \cdot \underline{x}\right) &= \underline{0} \\ \underline{\underline{A}}\left(\underline{w}, \hat{\underline{n}}_{ij}\right) &:= \partial\left(\hat{\underline{n}}_{ij} \cdot \underline{\underline{F}}^a\right) \big/ \partial \underline{w}, \end{aligned}$$

with the inter-cell normal flux vector

$$\begin{aligned} \hat{\underline{n}} \cdot \underline{\underline{F}}^a\left(\underline{w}\right) &= \left(\rho \hat{\underline{n}} \cdot \underline{u}, \rho \hat{\underline{n}} \cdot \underline{u}\,\underline{u} + p\hat{\underline{n}}, \rho \hat{\underline{n}} \cdot \underline{u}\, h_t\right)^{\mathrm{T}} = \dots \\ \dots &= \left(\hat{\underline{n}} \cdot \underline{\varpi}, \rho^{-1} \hat{\underline{n}} \cdot \underline{\varpi}\,\underline{\varpi} + p\left(\underline{w}\right)\hat{\underline{n}}, \rho^{-1} \hat{\underline{n}} \cdot \underline{\varpi}\left(\varepsilon_t + p\left(\underline{w}\right)\right)\right)^{\mathrm{T}}, \end{aligned}$$

the Jacobian matrix of the advective fluxes results in

$$\underline{\underline{A}}\left(\underline{w}, \hat{\underline{n}}\right) = \tag{3}$$

$$\begin{pmatrix} 0 & \hat{\underline{n}}^{\mathrm{T}} & 0 \\ -\hat{\underline{n}} \cdot \underline{u}\,\underline{u} + \partial_\rho p\left(\underline{w}\right)\hat{\underline{n}} & \underline{u} \otimes \hat{\underline{n}} + \hat{\underline{n}} \otimes \partial_{\underline{\varpi}} p\left(\underline{w}\right) + \hat{\underline{n}} \cdot \underline{u}\, \underline{\underline{I}} & \partial_{\varepsilon_t} p\left(\underline{w}\right)\hat{\underline{n}} \\ -\hat{\underline{n}} \cdot \underline{u}\left(h_t - \partial_\rho p\left(\underline{w}\right)\right) & h_t \hat{\underline{n}}^{\mathrm{T}} + \hat{\underline{n}} \cdot \partial_{\underline{\varpi}} p\left(\underline{w}\right) & \left(1 + \partial_{\varepsilon_t} p\left(\underline{w}\right)\right)\hat{\underline{n}} \cdot \underline{u} \end{pmatrix}.$$

The partial derivatives of the pressure function can be evaluated applying the chain rule

$$\begin{aligned} \partial_{\underline{w}} p\left(\underline{w}\right) &= \partial_{\underline{w}} p\left(\rho, e\left(\underline{w}\right)\right) = \partial_{\underline{w}} p\left(\rho, \rho^{-1}\varepsilon_t - \left(2\rho^2\right)^{-1} \underline{\varpi} \cdot \underline{\varpi}\right), \\ \partial_\rho p\left(\underline{w}\right) &= \partial_\rho p\left(\rho, e\right) - \rho^{-1} \partial_e p\left(\rho, e\right)\left(e_t - \underline{u} \cdot \underline{u}\right) \\ \partial_{\underline{\varpi}} p\left(\underline{w}\right) &= -\rho^{-1} \underline{u}\, \partial_e p\left(\rho, e\right) \\ \partial_{\varepsilon_t} p\left(\underline{w}\right) &= \rho^{-1} \partial_e p\left(\rho, e\right). \end{aligned}$$

The Roe-scheme, approximating the solution of the inter-cell Riemann problem (2), is given by

$$\left.\begin{aligned} \partial_t \underline{w} + \breve{\underline{\underline{A}}}\left(\underline{w}_i, \underline{w}_j, \hat{\underline{n}}_{ij}\right) \partial \underline{w} \big/ \partial\left(\hat{\underline{n}}_{ij} \cdot \underline{x}\right) &= \underline{0} \\ \underline{w}\left(\hat{\underline{n}}_{ij} \cdot \underline{x}, t\right)\Big|_{t=t_0} &= \begin{cases} \underline{w}_i\,, \hat{\underline{n}}_{ij} \cdot \underline{x} < 0 \\ \underline{w}_j\,, \hat{\underline{n}}_{ij} \cdot \underline{x} < 0 \end{cases} \end{aligned}\right\},$$

where $\breve{\underline{\underline{A}}}\left(\underline{w}_i, \underline{w}_j, \hat{\underline{n}}_{ij}\right)$ denotes the Roe-type linearization in $\hat{\underline{n}}_{ij}$ direction, which satisfies the properties defined by Roe [13]. In the present study the fundamental approach proposed by Cinnella [10] has been followed, in which the projection step [14] of most generalized Roe schemes is omitted. This projection might not lead to a physically consistent state for a two-phase flow [11]. With this simplification, Roe's [13] conservation property is generally not satisfied and the described linearization is strictly speaking not truly a Roe-type linearization, but results indicate that the resulting error does not significantly affect the computational outcomes [10] and in our experience only omitting the projection ensures physical consistency without further modifications when condensation occurs.

To finally calculate the numerical flux vector of the Roe scheme, the eigen-decomposition of the Jacobian matrix (3) is needed, which is omitted here for brevity. For the Roe averaged speed of sound, differently to Cinnella [10], we propose the direct calculation by the equation of state

$$\breve{a}^2 := a^2\left(\breve{\rho}, \breve{e}\right) = \partial_\rho p\left(\breve{\rho}, \breve{e}\right) + \breve{\rho}^{-2} p\left(\breve{\rho}, \breve{e}\right) \partial_e p\left(\breve{\rho}, \breve{e}\right)$$

to ensure consistency in the two-phase region.

To prevent the appearance of nonphysical solutions at sonic points, the Harten and Hyman [21] entropy fix is applied. The second order accuracy in space is achieved by a piecewise linear MUSCL-reconstruction [22] with a modified van Albada limiter. For performance and consistency reasons we propose a reconstruction based on the physical variables

$$\underline{w}_\pi := \left(\rho, \underline{u}, e\right),$$

for the general system (1).

Boundary Treatment

In turbomachines, computations must be performed on very small computational domains such that in contrast to external aerodynamics generally no undisturbed flow states exist at the boundaries. Therefore, application of far-field boundary conditions causes spurious, nonphysical reflections at the boundaries, which not only invalidate the calculated flow field but also result in its dependence on the position of the boundaries. To prevent this, non-reflecting boundary conditions have to be applied.

The non-reflecting boundary treatment of Saxer and Giles [2] with a one-dimensional characteristic reconstruction of boundary face values for cell-centered schemes proposed by Robens et al. [23] is adopted in the CFD solver TRACE. For the general equation of state approach utilized in this work, the inflow boundary treatment had to be extended. The changes of the circumferentially averaged characteristic values are determined by a one-step Newton-Raphson procedure

$$\Delta \underline{c} = -\partial \underline{c} / \partial \underline{r} \cdot \underline{r} \,, \tag{4}$$

with the residual

$$\underline{r} := \left(p\left(s(p,\rho) - s^{\mathrm{BC}}\right), \rho a\left(v - u\tan\beta^{\mathrm{BC}}\right), \ldots \right.$$
$$\left. \ldots, \rho a\left(v - u\tan\gamma^{\mathrm{BC}}\right), \rho\left(h_t(p,\rho) - h_t^{\mathrm{BC}}\right), \Delta c_5\right)^{\mathrm{T}}.$$

The $(\bullet)^{\mathrm{BC}}$ values are prescribed. In contrast to the ideal gas case the entropy $s = s(\rho, p)$ is used instead of some entropy related function and the total enthalpy is treated as a general equation of state $h_t = h_t(\rho, p)$.

Neglecting several terms which are zero in the converged limit [24], the Jacobian matrix in eq. (4) results in

$$\frac{\partial \underline{c}}{\partial \underline{r}} = Q^{-1} \begin{pmatrix} -\Gamma_1 Q & 0 & \cdots \\ -\Gamma_1\Gamma_2 \tan\beta^{\mathrm{BC}} & -\mathrm{Ma}_y \tan\beta^{\mathrm{BC}} + Q & \cdots \\ -\Gamma_1\Gamma_2 \tan\gamma^{\mathrm{BC}} & -\mathrm{Ma}_y \tan\gamma^{\mathrm{BC}} & \cdots \\ -2\Gamma_1\Gamma_2 & -2\,\mathrm{Ma}_y & \cdots \\ 0 & 0 & \cdots \end{pmatrix}$$
$$\begin{pmatrix} \cdots & 0 & 0 & 0 \\ \cdots & -\mathrm{Ma}_z \tan\beta^{\mathrm{BC}} & \tan\beta^{\mathrm{BC}} & (\Gamma_3 - \Gamma_2)\tan\beta^{\mathrm{BC}} \\ \cdots & -\mathrm{Ma}_z \tan\gamma^{\mathrm{BC}} + Q & \tan\gamma^{\mathrm{BC}} & (\Gamma_3 - \Gamma_2)\tan\gamma^{\mathrm{BC}} \\ \cdots & -2\,\mathrm{Ma}_z & 2 & 2(\Gamma_3 - \Gamma_2) + Q \\ \cdots & 0 & 0 & Q \end{pmatrix}$$

with

$$\Gamma_1 := a^2 \left(p\, \partial_\rho s(\rho,p)\big|_p\right)^{-1}$$
$$\Gamma_2 := \rho a^{-2}\, \partial_\rho h(\rho,p)\big|_p$$
$$\Gamma_3 := -\rho\, \partial_p h(\rho,p)\big|_\rho$$
$$Q := \rho\, \partial_p h(\rho,p)\big|_\rho + \Gamma_2 + \mathrm{Ma}_x + \mathrm{Ma}_y \tan\beta^{\mathrm{BC}} + \mathrm{Ma}_z \tan\lambda^{\mathrm{BC}}$$

and the Mach numbers $\mathrm{Ma}_{\underline{x}} := \underline{u}/a$.

For inviscid wall boundary conditions the treatment presented in [25] reformulated in physical variables is used, for no-slip adiabatic wall boundary conditions the treatment given in [26] is imposed.

RESULTS AND DISCUSSION

In this section, we present results of the developed solver for condensing steam flows in a de Laval nozzle geometry, a quasi-3D cascade and an idealized three-dimensional cascade geometry.

De Laval nozzle

The first configuration considered is the de Laval nozzle geometry (A) of Moore et al. [27]. For this quasi-3D calculation, the steady Euler equations are solved with an implicit pseudo time-stepping scheme, specifying a CFL-number of 50. Figure 1 shows the nozzle geometry and the computational gird with 316×30 cells.

As the flow is supersonic at the exit, the operating point is completely determined specifying the total inlet state with $p_t = 25000$ Pa and $T_t = 354.6$ K. A simple in- and outflow boundary treatment is applied. The initial field is created based on inlet density 0.1 kg/m^3, pressure 21000 Pa and axial velocity 240 m/s and outlet density 0.05 kg/m^3, pressure 15000 Pa and axial velocity 500 m/s.

In addition to a real-gas steam flow calculation based on the SBTL [1] equation of state, a calculation for the general system (1) closed by an ideal gas (IG) assumption and a calculation with an IAPWS-IF97 [3] based solver are conducted to demonstrate the capabilities of the proposed solution method. For every calculation 1000 iterations are done, the residuals are shown in figure 2. The IG and SBTL calculations can both be regarded as converged after 600 iterations, the IAPWS-IF97 calculation does not converge. The behavior of the IAPWS-IF97 formulation is due to the fact that the formulation cannot guarantee continuity in the thermodynamic state variables in proximity of the saturation lines. The SBTL calculation does not display such issues as the equation of state is continuously defined throughout the whole tabulated phase spcae.

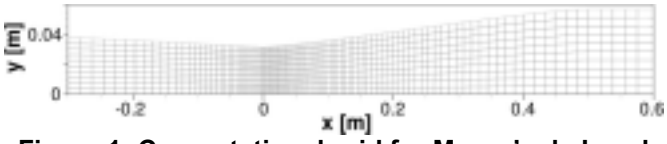

Figure 1: Computational grid for Moore's de Laval nozzle geometry omitting every third cell in each direction

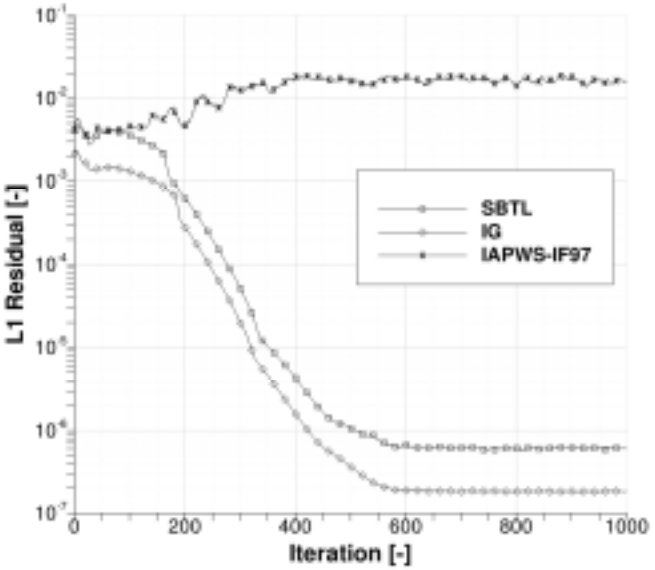

Figure 2: Residuals of the de Laval nozzle calculations

Figure 3 presents the volume averaged distributions of relative pressure and dryness fraction over the relative axial length of the nozzle in comparison with the experimental results of Moore et al. [27]. The calculation shows a good agreement with the measurement for the first points in axial direction. The following rise in pressure cannot be captured as no condensation model is implemented yet. However, from the computed dryness it can be seen that the Wilson line lies within this area. At the nozzle's exit the calculation advances deep into the wet steam region and reaches a dryness fraction of nearly 0.93.

Evaluating the computational speed reveals that the SBTL based real-gas steam calculation for this configuration is only a factor of 2.7 slower than a corresponding ideal gas calculation and 4.6 times faster than the IAPWS-IF97 based calculation (figure 4), showing the great potential of the presented method for high-performance calculations.

Turbine cascade

The second considered configuration is the turbine cascade experiment of White et al. [28] with the operating points (OPs) listed in table 1. For this configuration, the Reynolds-averaged Navier-Stokes equations are solved with a CFL-number of 10. For all calculations, the default entropy fix of 0.0075 is specified. Figure 5 shows the q3D computational mesh containing a total of 15040 internal cells.

At the inlet and outlet boundaries the extended non-reflecting boundary treatment is used based on area-averaged values. For the turbulence model turbulence intensity 0.01 and eddy length scale 0.00015 m are prescribed. The blade surface is an adiabatic, viscous wall. In y and z directions periodic boundary conditions are specified. The initial field for all computations is created based on inlet density 0.24 kg/m^3, pressure 40000 Pa and axial velocity 50 m/s and outlet density 0.16 kg/m^3, pressure 27000 Pa, axial velocity 80 m/s and circumferential velocity -188 m/s. For every calculation 5000 iterations are done, the residuals are shown in figure 6, the evaluation of the near wall resolution is given in table 2.

To demonstrate the effectiveness of the extended non-reflecting boundary treatment for condensing steam flows figure 7 shows results of computations with two different locations of the exit boundary plane, with the smaller domain corresponding to the standard setup. It can be clearly seen, that the non-reflecting boundary conditions allow the flow to adjust circumferentially to account for the presence of the

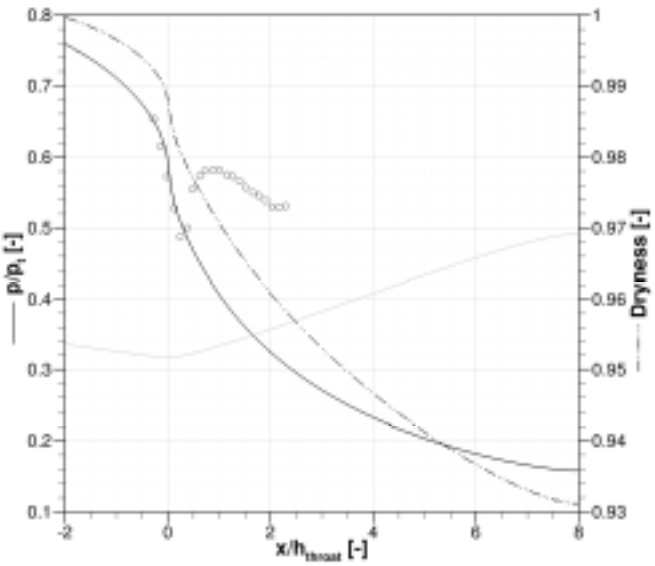

Figure 3: Area averaged axial distributions in the nozzle compared to measured pressure

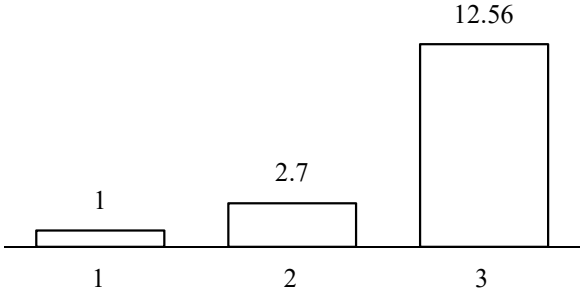

Figure 4: Evaluation of the computational costs for the de Laval nozzle calculations

Table 1: Total inlet states and outlet pressures for the considered OPs

OP	$p_{t,in}$ [bar]	$T_{t,in}$ [K]	p_{out} [bar]
L1	40300	354.0	16300
L2	40900	354.0	19400
L3	41700	357.5	20600

Table 2: Evaluation of the near wall resolution for the considered OPs

OP	$\max(y^+)$ [-]	$\overline{y^+}$ [-]
L1	6.32	2.82
L2	6.32	2.93
L3	6.36	2.97

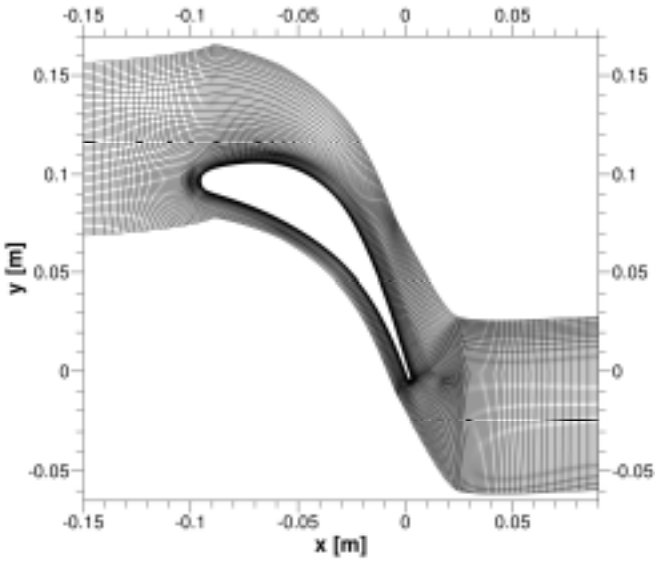

Figure 5: Computational grid for the turbine cascade

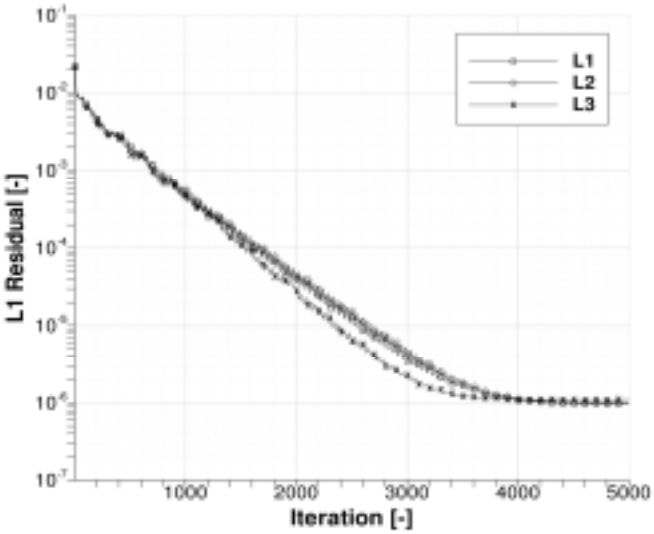

Figure 6: Residuals of the cascade calculations

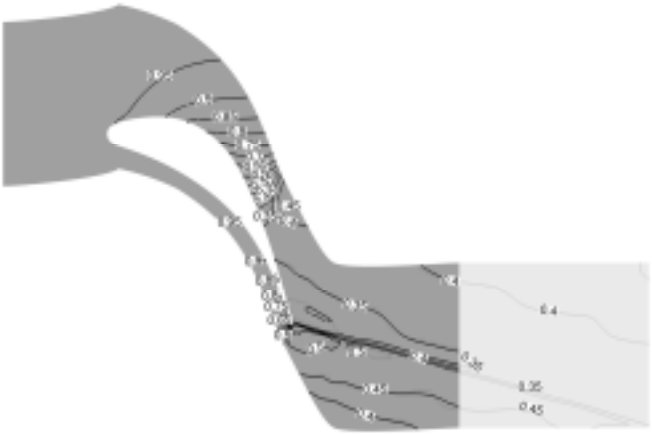

Figure 7: Pressure ratio of small and large domain calculations for the L1 OP

trailing edge and no unphysical reflections occur. Thus, the presented solution method can be employed for turbomachinery configurations involving real-gas effects.

The calculated pressure distribution on the blade is shown in figure 8 in comparison to the measurements for all considered operating points. The pressure side shows a very good agreement along the whole arc length. On the suction side condensation causes a pressure rise, most prominent in the L1 test case, that cannot be captured by the solutions of the considered model, as expected.

Idealized 3D Cascade configuration

To evaluate the computational speed of the proposed solver in a 3D configuration the presented computational mesh for the turbine cascade experiment of White et al. [28], shown in figure 5, is extruded in *z* direction by 100 cell layers, resulting in a mesh with 1.5 million internal cells. For this idealized configuration only the operating point L1 is considered and calculations for the general system (1) closed by the SBTL [1] and the ideal gas (IG) equation of state are

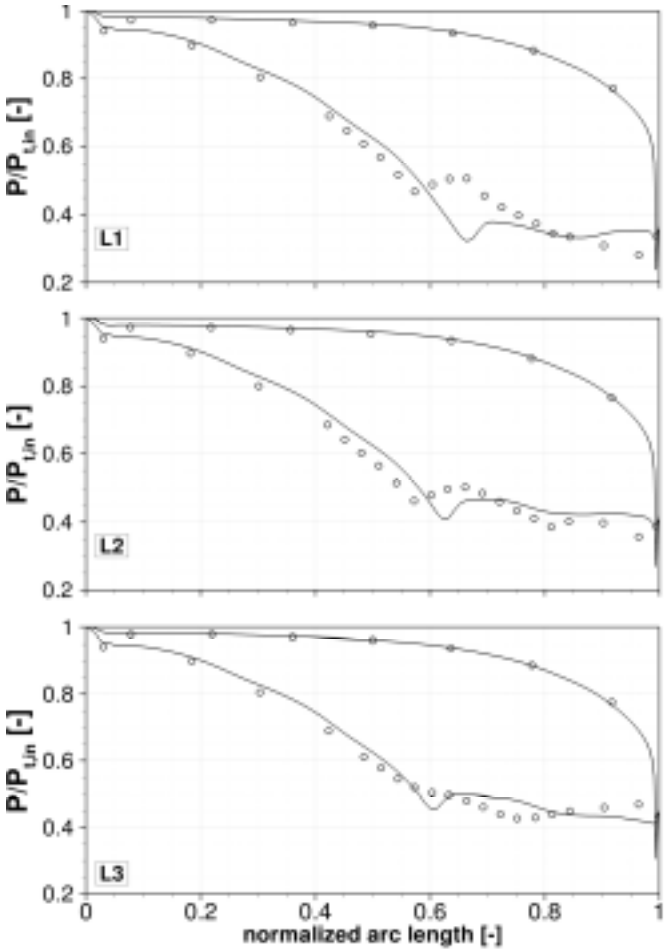

Figure 8: Calculated pressure ratio on the blade in comparison with the experimental data

conducted with the same setup as in the q3D case on 48 cores. The resulting residuals are given in figure 9.

Figure 10 shows radial area average and standard deviation of the pressure distribution on the blade in comparison with the experimental data. The obtained results correspond well with the q3D case; a variation of the radial distribution can only be found at about one third of the arc length on the suction side of the blade. In figure 11 an evaluation of the computational cost for this configuration is given, showing that the SBTL calculation is a factor of 5.2 slower than the ideal gas calculation.

CONCLUSIONS

The extension of the density-based turbomachinery CFD code TRACE to the computation of condensing steam flows utilizing the highly efficient Spline Based Table Lookup [1] method has been presented. The numerical fluxes are calculated based on an innovative generalized Roe-type scheme and an equilibrium assumption is invoked in the two-phase region at present time. A real-gas extension of the non-reflecting boundary treatment of Saxer and Giles [2] has been adopted.

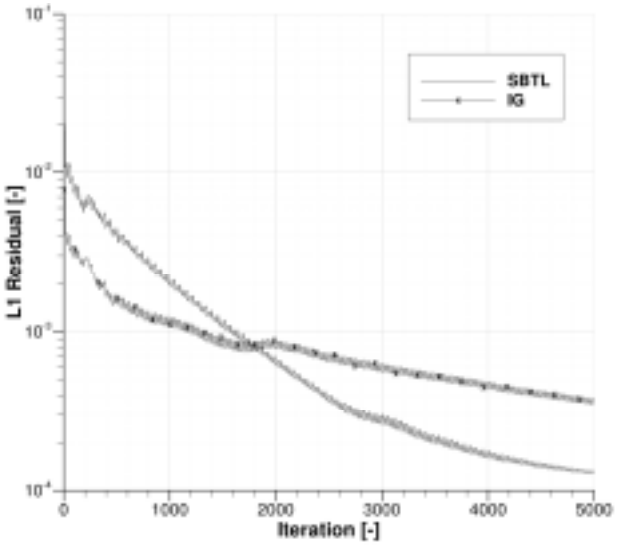

Figure 9: Residuals of 3D calculations

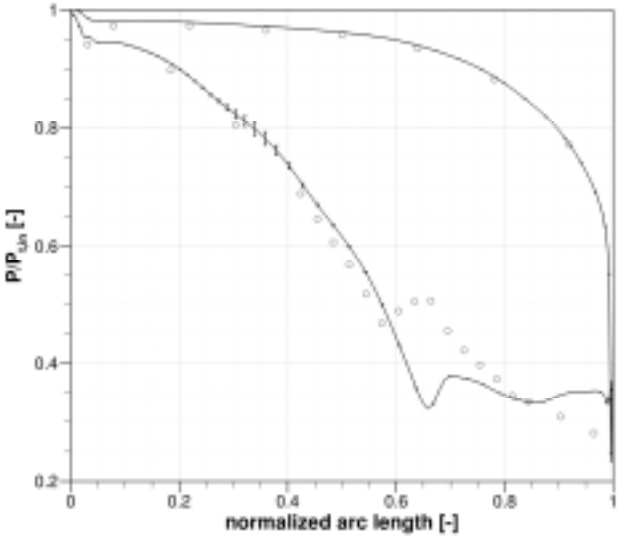

Figure 10: Radial area average and standard deviation of blade pressure in comparison to experimental data

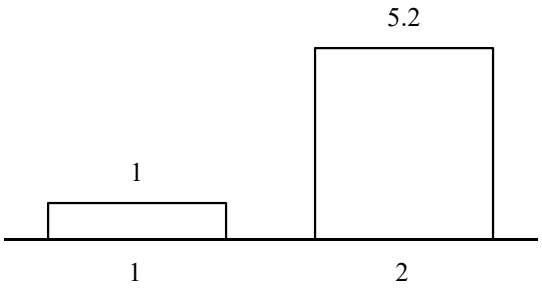

Figure 11: Evaluation of the computational costs for the idealized 3D cascade configuration

The capabilities and potential of the newly developed real-gas steam solver have been demonstrated in a de Laval nozzle geometry, a quasi-3D cascade and an idealized three-dimensional cascade geometry. In the de Laval nozzle case a speed-up of about 4.6 in computational time is gained compared to the industrial standard steam equation of state IAPWS-IF97 [3], only a factor of 2.7 slower than corresponding ideal gas calculations. In the 3D calculation, the SBTL based solver was only a factor of 5.2 slower than the ideal gas calculation. Due to these qualities, the developed solver has the potential for high-performance computations. Large eddy simulations of condensing steam flows in turbomachines and the implementation of a Lagrangian tracking algorithm to capture condensation effects are subjects of future research.

NOMENCLATURE

$\underline{\underline{I}}$	Identity tensor
$\underline{\underline{A}}$	Jacobian matrix of advective fluxes
$\breve{\underline{\underline{A}}}$	Roe-type linearization
$\underline{\underline{F}}^a$	advective fluxes
$\underline{\underline{F}}^d$	diffusive fluxes
T	temperature
a	equilibrium speed of sound
$\underline{c}$	vector of the characteristic variables
e	internal energy
e_t	total internal energy
h	enthalpy
h_t	total enthalpy
$\hat{\underline{n}}$	outward unit normal vector
$\hat{\underline{n}}_{ij}$	outward unit normal vector of S_{ij}
p	pressure
$\underline{q}$	heat flux vector
$\underline{r}$	residual vector
S_{ij}	inter-cell boundary between cells i and j
$\underline{u}$	velocity vector
$\underline{w} := (\rho, \underline{\varpi}, \varepsilon_t)^{\mathrm{T}}$	vector of conservative variables
$\underline{w}_\pi := (\rho, \underline{u}, e)$	vector of physical variables
$\underline{x}$	vector of space variables
β, γ	flow angles
η	molecular viscosity
λ	thermal conductivity coefficient
ρ	density
$\underline{\underline{\tau}}$	viscous shear stress tensor
$(\bullet)_i$	cell mean values of cell i
$(\bullet)_l$	subscript for saturated liquid
$(\bullet)_v$	subscript for superheated vapor
$(\bullet)_m$	subscript for saturated mixture
$(\bar{\bullet})$	Reynolds-averaged quantity
$(\tilde{\bullet})$	Favre-averaged quantity
$(\breve{\bullet})$	Roe-averaged quantity
$(\bullet)^*$	modified values in RANS equations
$(\bullet)^t$	turbulent quantity
$(\bullet)^{\mathrm{BC}}$	boundary prescribed value

ACKNOWLEDGMENTS

This research has been financially supported by the DFG in the framework of the Excellence Initiative, Darmstadt Graduate School of Excellence Energy Science and Engineering (GSC 1070).

REFERENCES

[1] Kunick M, Kretzschmar H-J, Mare F di, and Gampe U, "CFD Analysis of steam turbines with the IAPWS standard on the Spline-Based Table Look-Up Method (SBTL) for the fast calculation of real fluid properties", Proceedings of ASME Turbo Expo 2015: Turbine Technical Conference and Exposition, 2015

[2] Saxer A and Giles M, "Quasi-three-dimensional nonreflecting boundary conditions for Euler equations calculations", *J. Propuls. Power*, 9(2), 1993, pp 263–271

[3] Wagner W and Kretzschmar H-J, "International Steam Tables", Berlin, Heidelberg: Springer Berlin Heidelberg, 2008

[4] Gerber AG and Kermani MJ, "A pressure based Eulerian–Eulerian multi-phase model for non-equilibrium condensation in transonic steam flow", *Int. J. Heat Mass Transf.*, 47(10–11), 2004, pp 2217–2231

[5] Gerber AG, Sigg R, Völker L, Casey MV, and Sürken N, "Predictions of non-equilibrium phase transition in a model low-pressure steam turbine", *Proc. Inst. Mech. Eng. Part J. Power Energy*, 221(6), 2007, pp 825–835

[6] Dykas S, "Numerical calculation of the steam condensing flow", *Task Q.*, 5(4), 2001, pp 519–535

[7] Dykas S and Wróblewski W, "Two-fluid model for prediction of wet steam transonic flow", *Int. J. Heat Mass Transf.*, 60, 2013, pp 88–94

[8] Kügeler E, "Numerisches Verfahren zur genauen Analyse der Kühleffektivität filmgekühlter Turbinenschaufeln", Köln: DLR, Bibliotheks- und Informationswesen, Dissertation, DLR Forschungsbericht 2005-11, 2005

[9] Mottura L, Vigevano L, and Zaccanti M, "An Evaluation of Roe's Scheme Generalizations for Equilibrium Real Gas Flows", *J. Comput. Phys.*, 138(2), 1997, pp 354–399

[10] Cinnella P, "Roe-type schemes for dense gas flow computations", *Comput. Fluids*, 35(10), 2006, pp 1264–1281

[11] Toumi I, "A weak formulation of Roe's approximate Riemann solver", *J. Comput. Phys.*, 102(2), 1992, pp 360–373

[12] Guardone A and Vigevano L, "Roe Linearization for the van der Waals Gas", *J. Comput. Phys.*, 175(1), 2002, pp 50–78

[13] Roe PL, "Approximate Riemann solvers, parameter vectors, and difference schemes", *J. Comput. Phys.*, 43(2), 1981, pp 357–372

[14] Liou M-S, Leer BV, and Shuen J-S, "Splitting of inviscid fluxes for real gases", *J. Comput. Phys.*, 87(1), 1990, pp 1–24

[15] Wilcox DC, "Reassessment of the scale-determining equation for advanced turbulence models", *AIAA J.*, 26(11), 1988, pp 1299–1310

[16] Boussinesq J, "Théorie de l'écoulement tourbillonnant et tumultueux des liquides dans les lits rectilignes a grande section", Paris, Gauthier-Villars et fils, 1897

[17] Godlewski E and Raviart P-A, "Numerical Approximation of Hyperbolic Systems of Conservation Laws", Springer Science & Business Media, 1996

[18] Barth T, "Analysis of implicit local linearization techniques for upwind and TVD algorithms", AIAA 87-0595, 1987

[19] Tysinger T and Caughey D, "Implicit multigrid algorithm for the Navier-Stokes equations", AIAA 91-0242, 1991

[20] Godunov S, "A finite difference scheme for numerical computation of the discontinuous wave solutions of equations of fluid dynamics", *Math Sb*, 47, 1959, pp 271–306

[21] Harten A and Hyman JM, "Self adjusting grid methods for one-dimensional hyperbolic conservation laws", *J. Comput. Phys.*, 50(2), 1983, pp 235–269

[22] van Leer B, "Towards the ultimate conservative difference scheme. V. A second-order sequel to Godunov's method", *J. Comput. Phys.*, 32(1), 1979, pp 101–136

[23] Robens S, Jeschke P, Frey C, Kügeler E, Bosco A, and Breuer T, "Adaption of Giles Non-Local Non-Reflecting Boundary Conditions for a Cell-Centered Solver for Turbomachinery Applications", ASME Turbo Expo 2013: Turbine Technical Conference and Exposition, 2013

[24] Giles M, "UNSFLO: A numerical method for the calculation of unsteady flow in turbomachinery", Gas Turbine Laboratory, Massachusetts Institute of Technology, 1991

[25] Whitfield D and Janus J, "Three-dimensional unsteady Euler equations solution using flux vector splitting", AIAA 84-1552, 1984

[26] Toro EF, "A fast riemann solver with constant covolume applied to the random choice method", *Int. J. Numer. Methods Fluids*, 9(9), 1989, pp 1145–1164

[27] Moore MJ, Walters PT, Crane RI, and Davidson BJ, "Predicting the fog drop size in wet steam turbines", *Wet Steam*, 4, 1973, pp 101–109

[28] White AJ, Young JB, and Walters PT, "Experimental Validation of Condensing Flow Theory for a Stationary Cascade of Steam Turbine Blades", *Philos. Trans. R. Soc. Lond. Math. Phys. Eng. Sci.*, 354(1704), 1996, pp 59–88